A Recursive Filter for Noise Reduction in Statistical Iterative Tomographic Imaging

Jean-Baptiste Thibault[a], Charles A. Bouman[b], Ken D. Sauer[c], and Jiang Hsieh[a]

[a]Applied Science Laboratory, GE Healthcare Technologies, W-1180, 3000 N Grandview Bvd, Waukesha, WI 53188;
[b]School of Electrical Engineering, Purdue University, West Lafayette, IN 47907-0501;
[c]Department of Electrical Engineering, 275 Fitzpatrick, University of Notre Dame, Notre Dame, IN 46556-5637

ABSTRACT

Computed Tomography (CT) screening and pediatric imaging, among other applications, demand the development of more efficient reconstruction techniques to diminish radiation dose to the patient. While many methods are proposed to limit or modulate patient exposure to x-ray at scan time, the resulting data is excessively noisy, and generates image artifacts unless properly corrected. Statistical iterative reconstruction (IR) techniques have recently been introduced for reconstruction of low-dose CT data, and rely on the accurate modeling of the distribution of noise in the acquired data. After conversion from detector counts to attenuation measurements, however, noisy data usually deviate from simple Gaussian or Poisson representation, which limits the ability of IR to generate artifact-free images. This paper introduces a recursive filter for IR, which conserves the statistical properties of the measured data while pre-processing attenuation measurements. A basic framework for inclusion of detector electronic noise into the statistical model for IR is also presented. The results are shown to successfully eliminate streaking artifacts in photon-starved situations.

Keywords: Computed tomography, bias correction, iterative reconstruction, noise modeling

1. INTRODUCTION

The objective of Computed Tomography (CT) is to reconstruct the cross-section of an object by measuring the line integrals of attenuation through the object for a number of projection angles. For example, consider an object with a two-dimensional cross-section specified by $\mu(x, y)$, where x, y specify the position along two orthogonal axis. Here, $\mu(x, y)$ represents the density of the object's cross-section, which specifies the rate at which photons (or other particles) are absorbed as they pass through the object.

In order to reconstruct cross-sectional images, it is necessary to measure the projections through the object at various angles and positions. A projection angle at angle θ and displacement t can be expressed as

$$p(\theta, t) = \int_{-\infty}^{\infty} \mu\left(-z\sin\theta + t\cos\theta, z\cos\theta + t\sin\theta\right) dz \tag{1}$$

as illustrated in Figure 1.

It is generally not possible to measure the projection $p(\theta, t)$ directly. Instead, one measures the photons at the detector that pass through the object along the line of the projection. The measurement at angle θ and displacement t can be expressed as the function $\lambda(\theta, t)$, which is proportional to the number of detected photons. Generally, $\lambda(\theta, t)$ is corrupted by a number of sources of noise and distortion. This noise can be photon counting noise that is often modeled by a Poisson distribution, or it can be additive noise, that is often modeled by

Further author information: (Send correspondence to J.B.T.)
J.B.T.: E-mail: jean-baptiste.thibault@med.ge.com, Telephone: 1 262 312 7404
C.A.B.: E-mail: bouman@purdue.edu, Telephone: 1 765 494 0340
K.D.S.: E-mail: sauer@nd.edu, Telephone: 1 574 631 6999
J.H.: E-mail: jiang.hsieh@med.ge.com, Telephone: 1 262 312 7635

Computational Imaging IV, edited by Charles A. Bouman, Eric L. Miller, Ilya Pollak,
Proc. of SPIE-IS&T Electronic Imaging, SPIE Vol. 6065, 60650X, © 2006 SPIE-IS&T · 0277-786X/06/$15

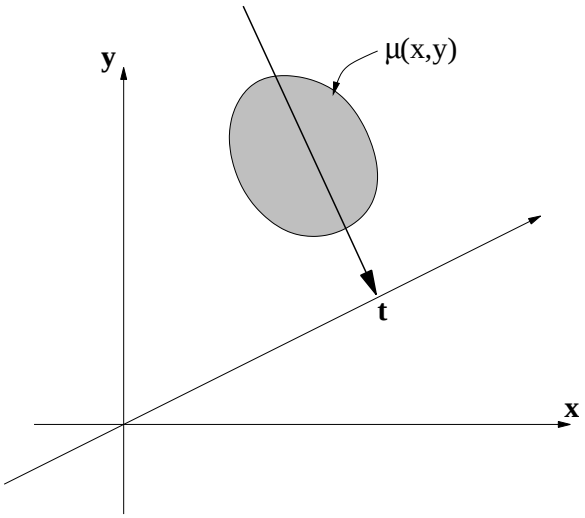

Figure 1. Single projection through the object for view angle θ and displacement t.

additive Gaussian noise. However, it is usually the case that the expected value of $\lambda(\theta, t)$ is related to the desired projection by the equation

$$\bar{\lambda}(\theta, t) = E[\lambda(\theta, t)] = \lambda_T \exp\left(-p(\theta, t)\right), \tag{2}$$

where $E[\cdot]$ denotes the expectation, $\bar{\lambda}(\theta, t)$ denotes the expected value of $\lambda(\theta, t)$, and λ_T denotes the number of photons which are impinging on the object from the photon source. In practice, the value of λ_T may vary with the projection, but in this discussion we assume without loss of generality that λ_T is constant. For purposes of explanation, we also use the exponential function; however, this exponential function may sometimes be replaced with another non-linearity that more accurately models the actual attenuation. Generally, any such non-linearity must map values of $p(\theta, t)$ to positive values of $\bar{\lambda}(\theta, t)$, and must be an invertible function.

Given equation (2), the desired projections may be computed from the expected measurements using the relationship

$$p(\theta, t) = -\log\left(\frac{\bar{\lambda}(\theta, t)}{\lambda_T}\right). \tag{3}$$

So from equation (3), it can be seen that the projections can be determined once the value of $\bar{\lambda}(\theta, t)$ is known. The difficulty in applying equation (3) is that the value of $\bar{\lambda}(\theta, t)$ is not known since only the noisy value of $\lambda(\theta, t)$ can be directly measured. There are two major sources of noise in $\lambda(\theta, t)$: photon statistics noise and electronic noise. The former corresponds to quantum noise related to the mechanism of interaction of x-ray with matter through absorption, Compton effect, and pair production,[1] and often dominates the distribution at usual scan techniques. The latter originates in the data acquisition system formed by the x-ray detector, analog-to-digital converters, encoders, and cables, and comes mainly from dark currents in the electronics, interference noise from inter-connecting cables, and many other sources. In scan techniques aimed at low-dose tomographic imaging, electronic noise certainly becomes non-negligible and affects measurements in a way which makes processing more difficult and risks degradation of the reconstructed images.

One approach to this problem is to use the approximation $\bar{\lambda}(\theta, t) \cong \lambda(\theta, t)$. If $\bar{\lambda}(\theta, t)$ is large, such as for high scanning techniques, this approximation is good since in this case the value of the signal is large compared to the level of noise. However, if the object being imaged is very dense or large, then the attenuation may be very great, and the value of $\bar{\lambda}(\theta, t)$ will be very small. In this case, the measured value of $\lambda(\theta, t)$ may have a large percentage error, or may even be negative, which conflicts with equation (3). This is usually due to the fact that the electronic noise in the CT system becomes significant as compared to the photon statistical noise. If $\lambda(\theta, t)$ is negative, the approximation $\bar{\lambda}(\theta, t) \cong \lambda(\theta, t)$ cannot be used because it would require that the logarithm of a negative number be computed in equation (3). Simple methods of dealing with this problem such as simply

zeroing the negatives, or replacing them with absolute values $\bar{\lambda}(\theta,t) \cong |\lambda(\theta,t)|$ to avoid generating artifacts due to large numbers of measurements clipped to zero, allow processing through equation (3), but corrupt the true statistical nature of the data and introduce negative bias in the reconstruction.

A second possible approach consists of taking many measurements of $\lambda(\theta,t)$ and computing the statistical average of those contributions to form the data set used for reconstruction. The noise in different measurements is generally independent, so by averaging one can obtain an approximation of the desired mean $\bar{\lambda}(\theta,t)$. However, this approach has a number of important disadvantages to practical use. First, it requires more time to perform the necessary acquisitions since $\lambda(\theta,t)$ must be measured multiple times. More importantly, it exposes the object to more harmful radiation; in human patient medical tomography, greater exposure to x-ray ionizing radiation may result in greater health risk, which is undesirable.

A third approach, representative of techniques often used in practice in pre-processing data for conventional reconstruction methods such as Filtered Back-Projection[2] (FBP), is to smooth neighboring values of $\lambda(\theta,t)$. Let $\lambda(i,j)$ denote the measured value for the i^{th} angle (i.e. the variable θ) and the j^{th} displacement (i.e. the variable t). Then one may apply a smoothing filter to $\lambda(i,j)$ which averages values which have nearly equal angles and displacements to produce a smoothed version of the measurement denoted by $\hat{\lambda}(i,j)$.[3] One may then use the approximation $\bar{\lambda}(\theta,t) \cong \hat{\lambda}(\theta,t)$. This smoothing filter can reduce the noise by averaging values with different noise samples, but has a number of disadvantages. It does not necessarily guarantee that the resulting smoothed value is positive since it might happen that a group of negative values fall near one another in the data. The averaging process also tends to blur the resolution of the reconstruction in regions that do not require averaging in the high signal-to-noise projections. Finally, the process may not preserve the physically accurate statistical nature of the data: corrupting the mean value of local regions in the measurements can lead to bias in the reconstruction, and shading artifacts in images.

Other approaches have been proposed to directly account in the processing for the distribution of detector counts including both quantum photon noise and detector readout noise, by considering mixed additive Poisson-Gaussian models.[4] Although, these techniques were investigated successfully, particularly for image restoration, such hybrid models for conversion from detector counts to projection attenuation measurements in CT can be used only at the cost of significant additional complexity in the reconstruction.

In this work, we introduce a simple recursive method for estimating $\bar{\lambda}(\theta,t)$ from $\lambda(\theta,t)$ which respects the true nature of the distribution of the measurement data for processing in equation (3) prior to reconstruction. In particular, preserving the local mean of the data is important to avoid introducing bias in the reconstruction. The technique we propose is specifically designed for iterative reconstruction by statistical modeling.[5] For such techniques, the quality of the noise modeling in the projection data is critical to image quality. Therefore, we also present in this paper the development of accurate noise modeling for statistical iterative reconstruction for low-dose imaging which accounts for electronic noise distribution, and introduce a similar iterative formulation of the bias correction filter as an alternative to the recursive method proposed above.

Section 2 details the proposed recursive filter to estimate $\bar{\lambda}(\theta,t)$ with high statistical fidelity to $\lambda(\theta,t)$ before applying equation (3). Section 3 introduces the statistical formulation of the reconstruction problem which can be solved iteratively, and focuses especially on developing a noise model which includes electronic noise. The iterative solution to the reconstruction problem also leads to an analogous method of iterative bias correction, in which the causal filter of section 2 can be replaced by a non-causal iterative filter we derive in section 4 for possibly improved results. Section 5 finally presents the application of the causal filter to phantom data, indicating promising outcomes for practical application.

2. POSITIVE BIAS CORRECTION

We introduce here a non-linear filtering process in one, two, or three dimensions, that smoothes only the low signal-to-noise measurements in $\lambda(\theta,t)$, while preserving the local average of the projection measurements and insuring that all resulting values are positive and ready for processing through equation (3) and subsequent iterative reconstruction.

Such local filtering methods have been derived for different applications in the past, for instance in the field of digital half-toning. A good example is the Floyd-Steinberg[6] error diffusion algorithm. The function of this

algorithm is to generate binary patterns whose local mean are nearly equal to the local mean of an image to be rendered, by means of displaying on a screen or printing it. Error diffusion operates by dispersing the error produced by binarization of pixels that have not yet been processed. Other methods, such as Direct Binary Search[7] (DBS) have been developed for digital half-toning and disperse the errors generated by binarization to all surrounding pixels. In some cases, these algorithms can be viewed as distributing the errors non-causally to both pixels that have not been processed and also pixels that have been processed. This type of algorithm is usually iterative by nature because of the fact that past pixels are affected by the processing of a present pixel. Generally, these iterative digital half-toning methods yield higher quality results than simpler techniques, but at the cost of additional computation, which is mitigated in practice by the use of specialized hardware in copiers, printers, etc.

Here, we apply a similar concept to the pre-processing of projection data for tomographic imaging, to specify the operation of a causal mean-preserving filter (MPF) on data corrupted by quantum and electronic noise. First, a non-linear function must be chosen to map any real valued input λ to strictly positive values. It is desirable that such a function does not significantly change positive values in $\lambda(\theta, t)$. These usually correspond to higher signal-to-noise ratios in the measurement data and pose no particular problem in the negative logarithm operation. Noise distribution for such data can be modeled as part of the statistical formulation for iterative reconstruction. Generally, it is best to use a strictly increasing monotone function, for instance:

$$g(\lambda) = \hat{\sigma} \log \left(\exp(\lambda/\hat{\sigma}) + 1 \right), \tag{4}$$

where $\hat{\sigma}$ is a parameter that can be tuned for best performance. This is accompanied by the choice of normalized weighting coefficients, for instance:

$$w_1 = 7/16, w_2 = 1/16, w_3 = 5/16, w_4 = 3/16. \tag{5}$$

With this initiation, the MPF filter works recursively to compute a new array $\tilde{\lambda}(i, j)$ from the measurements $\lambda(i, j)$. We refer to each position (i, j) in the 2-D array as a detector element (for each projection angle θ and displacement t). First, the values of a new array are initialized to the values of the measurement for all elements (i, j):

$$\tilde{\lambda}(i, j) \leftarrow \lambda(i, j), \tag{6}$$

where the symbol $\leftarrow$ denotes that the values of $\lambda(i, j)$ are assigned to the array $\tilde{\lambda}(i, j)$. Next, the values of the elements (i, j) are considered in some order, such as raster or serpentine, defined to sequentially visit each element once at each iteration. For each such position (i, j), the non-linear transformation in equation (4) is applied to compute a strictly positive value for $\tilde{\lambda}(i, j)$:

$$\tilde{\lambda}(i, j) \leftarrow g\left(\tilde{\lambda}(i, j) \right). \tag{7}$$

Next, the error is computed as

$$\epsilon \leftarrow g\left(\tilde{\lambda}(i, j) \right) - \tilde{\lambda}(i, j) \tag{8}$$

and the negative of this error is distributed to elements that have not yet been processed. We choose to use standard dispersion such as illustrated in Figure 2 (a) when processing from left to right:

$$\begin{aligned} \tilde{\lambda}(i, j+1) &\leftarrow \tilde{\lambda}(i, j+1) - w_1 \epsilon \\ \tilde{\lambda}(i+1, j+1) &\leftarrow \tilde{\lambda}(i+1, j+1) - w_2 \epsilon \\ \tilde{\lambda}(i+1, j) &\leftarrow \tilde{\lambda}(i+1, j) - w_3 \epsilon \\ \tilde{\lambda}(i+1, j-1) &\leftarrow \tilde{\lambda}(i+1, j-1) - w_4 \epsilon \end{aligned} \tag{9}$$

and such as illustrated in Figure 2 (b) when processing from right to left:

$$\begin{aligned} \tilde{\lambda}(i, j-1) &\leftarrow \tilde{\lambda}(i, j-1) - w_1 \epsilon \\ \tilde{\lambda}(i+1, j-1) &\leftarrow \tilde{\lambda}(i+1, j-1) - w_2 \epsilon \\ \tilde{\lambda}(i+1, j) &\leftarrow \tilde{\lambda}(i+1, j) - w_3 \epsilon \\ \tilde{\lambda}(i+1, j+1) &\leftarrow \tilde{\lambda}(i+1, j+1) - w_4 \epsilon \end{aligned} \tag{10}$$

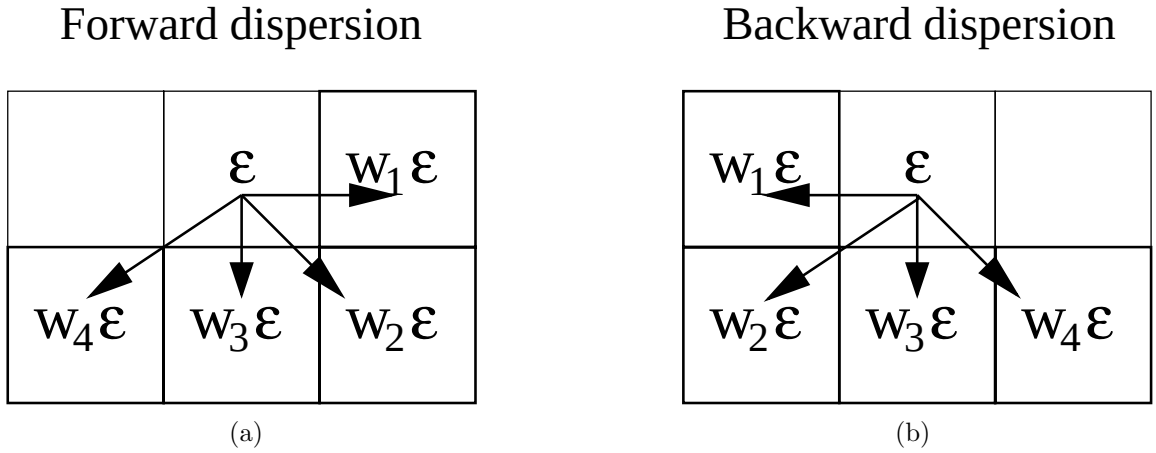

Figure 2. Forward (a) and backward (b) error dispersion for bias correction.

After the error is propagated to the local neighborhood of element (i, j), a new element is selected among the set of elements yet to be visited, and the process described in equations (7), (8), (9), and (10) is repeated until all the elements have been processed.

Note that for multi-slice detector arrays, the processing becomes three-dimensional, across projection angles, detector channels, and detector rows. The filtering may be applied as a number of 2-D processing steps as shown in the above example, either in rows and channels for each projection angle, or better in projection views and channels for each detector row, so as to minimize the residual error. Or a similar process may be developed for error dispersion directly in three dimensions, which we have not experimented with.

The operation of this causal MPF is analogous to the operation of an error diffusion filter used in digital half-toning in that it is designed to match the local means of the measurement data $\lambda(i, j)$ and the processed input $\tilde{\lambda}(i, j)$, but it differs in two significant ways. First, it uses a non-linearity $g(\lambda)$ that is designed to insure that the output is a continuous positive value rather than being designed to quantize the output. Second, it is used to process density measurements, rather than to digitally render an image.

3. ELECTRONIC NOISE MODELING FOR STATISTICAL ITERATIVE RECONSTRUCTION

Iterative methods for CT image reconstruction have originally been introduced on the very first CT scanners, with such methods as algebraic reconstruction techniques (ART),[8] which iteratively change subsets of image values in an attempt to reduce error. A different class of methods allows the inclusion of more realistic descriptions of the true physical processes involved in x-ray scanning.[9] Image reconstruction can be defined in a statistically optimal sense by developing appropriate models of the distribution of noise in the projection data, and accounting for the variance in the measurements.

Let $\mathbf{r}$ be the vector of x-ray densities of elements of the three-dimensional imaged object, $\mathbf{p}$ the actual projection measurements as defined in section 1. In general, the optimization problem in iterative reconstruction can be expressed as

$$\hat{\mathbf{r}} = \arg\min_{\mathbf{r}} \left\{ G\left(\mathbf{p} - F(\mathbf{r})\right) + U(\mathbf{r}) \right\}, \tag{11}$$

In equation (11), $F(\mathbf{r})$ is a transformation of the image space $\mathbf{r}$ in a manner representative of the CT system. The model $F(\mathbf{r})$ includes the precise geometry of the scan pattern and the source/detector structure. Frequently, a linear model of the form $\mathbf{p} = \mathbf{A}\mathbf{r} + \mathbf{n}$ is used, where the noise values in $\mathbf{n}$ represent random fluctuations of the measurement about its mean. $U(\mathbf{r})$ is a regularization function that stabilizes the objective by enforcing local penalties on the image $\mathbf{r}$. The function $G(\cdot)$ is our focus of interest here. It represents a measure of statistical confidence in the data, and can be derived from the distribution of the projections. A good approximation for

the x-ray transmission problem is based on a second order Taylor series expansion of the Poisson distribution of the measurement counts,[10] and yields the quadratic form

$$G\left(\mathbf{p}-F(\mathbf{r})\right) \approx \frac{1}{2}\left(\mathbf{p}-F(\mathbf{r})\right)^T \mathbf{D}\left(\mathbf{p}-F(\mathbf{r})\right), \tag{12}$$

where $\mathbf{D}$ is a diagonal matrix. Its coefficients d_i are proportional to detector counts, which are Maximum Likelihood estimates of the inverse of the variance of the projection measurements $\frac{1}{\sigma_p^2}$.[10,11] Recall from equation (3) the relation between projection data p_i and detector count λ_i for measurement index i to obtain

$$d_i \sim \lambda_i = \lambda_T e^{-p_i} \cong \frac{1}{\sigma_p^2}. \tag{13}$$

This formulation can be extended to explicitly model electronic noise in the reconstruction process, in a manner related to the recursive filter designed in section 2 to preserve the local mean in the projection data. In reality, the combination of x-ray quantum noise and detector electronic noise yields a compound additive Poisson-Gaussian distribution. This must be accounted for in the noise modeling so as to minimize related artifacts. Introduce $\bar{\lambda}_i$ as the average detector count, and $\bar{p}_i$ as the true projection data. Then

$$\begin{aligned} p_i &= \log\left(\frac{\lambda_T}{\bar{\lambda}_i}\right) + \log\left(\frac{\bar{\lambda}_i}{\lambda_i}\right) \\ &= \bar{p}_i - \log\left(\frac{\lambda_i}{\bar{\lambda}_i}\right) \\ &\cong \bar{p}_i + \left(1 - \frac{\lambda_i}{\bar{\lambda}_i}\right). \end{aligned} \tag{14}$$

Equation (14) provides a linear approximation of the relationship between projection data and detector counts, and leads to a related description of their respective variances. Let σ_λ the standard deviation of the x-ray photons arriving at the detector. For a Poisson process, the variance is equal to the mean, so $\sigma_\lambda^2 = \bar{\lambda}_i$. Since electronic noise is an additive process with standard deviation σ_n, the variance in the total detector counts is $\sigma_\lambda^2 + \sigma_n^2$. Therefore, under the more physically accurate assumption of a compound Poisson-Gaussian distribution for the detector counts, we obtain from equation (14) a better estimate of the variance in the projection attenuation measurements:

$$\hat{\sigma}_p^2 \cong \left(\sigma_\lambda^2 + \sigma_n^2\right)\left(\frac{1}{\bar{\lambda}_i}\right)^2 \tag{15}$$

Approximately the inverse of the variance in the projection measurements is used for calculating the coefficients d_i of the diagonal weighting matrix $\mathbf{D}$, so

$$\begin{aligned} d_i &\sim \frac{1}{\hat{\sigma}_p^2} \cong \frac{\bar{\lambda}_i^2}{\bar{\lambda}_i + \sigma_n^2} \\ &\cong \frac{\lambda_T^2 e^{-2p_i}}{\lambda_T e^{-p_i} + \sigma_n^2} \\ &\cong \lambda_T e^{-p_i}\left(\frac{e^{-p_i}}{e^{-p_i} + \frac{\sigma_n^2}{\lambda_T}}\right). \end{aligned} \tag{16}$$

This new formulation incorporates electronic noise into the statistical modeling for iterative reconstruction as in (11). The quantity $\frac{\sigma_n^2}{\lambda_T}$ may be viewed as the ratio between quantum detector noise and photon noise. To determine this parameter, a first order approximation might be to relate this quantity to the rays of maximum attenuation in the projection data:

$$\frac{\sigma_n^2}{\lambda_T} \equiv e^{-p_{\max}} \tag{17}$$

but this may not apply in the general case since it does not take into account the signal-to-noise ratio. Instead, experimental means of observation of the standard deviation of electronic noise in the DAS may be needed.

Equation (16) assumes working directly from the pre-corrected projection measurements $\mathbf{p}$. One might argue that the statistical model may gain in accuracy by directly using the raw count random measurements λ_i corrected only by detector offset calibration measurements, in which case $\mathbf{D}$ becomes

$$d_i = \lambda_i \left(\frac{\lambda_i}{\lambda_i + \sigma_n^2} \right). \tag{18}$$

Offset calibration is usually performed before each scan by taking measurements with x-ray off in order to determine temporal variations due to changes in temperature.

The statistical formulation formed by the combination of equations (11), (12), and (16) or (18) requires an iterative solution to obtain the most likely image estimates satisfying the optimization criteria. We use the Iterative Coordinate Descent[10] (ICD) algorithm to optimize the estimates. The ICD algorithm works by reducing the N-dimensional optimization problem to a series of one-dimensional greedy updates, solving for one image element at step $(n+1)$ based on the full state after step (n):

$$\hat{r}_j^{(n+1)} = \arg\min_{r_j \geq 0} \left\{ \sum_i \frac{d_i}{2} \left(p_i - \mathbf{A}_{i*}\mathbf{r}^{(n)} + A_{ij}(r_j^{(n)} - r_j) \right)^2 + U(\mathbf{r}^{(n)}, r_j) \right\}. \tag{19}$$

The ICD algorithm has been shown to converge quite rapidly compared to various other iterative techniques for computed tomography.[12] Interestingly, it also easily enforces positivity constraints on the solution.

4. ITERATIVE BIAS CORRECTION

Much in the way that the ICD algorithm operates on single voxel elements to iteratively obtain optimal *positive* estimates by equation (19), an iterative filter for bias correction can be derived to replace the causal MPF of section 2. The idea is to introduce a statistical model for the detector count elements which guarantees positivity, and ensures that the corresponding projection data computed by equation (3) are little affected. The Iterative Positive Filter (IPF) takes the form:

$$\hat{\tilde{\lambda}}(i,j) = \arg\min_{\tilde{\lambda}>0} \left\{ \sum_{i,j} \left(\lambda(i,j) - \tilde{\lambda}(i,j) \right)^2 + \gamma \sum_{i,j,k,l} b_{i-k,j-l} \left(\log\left(\tilde{\lambda}(k,l) \right) - \log\left(\tilde{\lambda}(i,j) \right) \right)^2 \right\}. \tag{20}$$

In equation (20), $\tilde{\lambda}(i,j)$ is the processed output of the IPF algorithm, $\sum_{i,j} b_{i,j} = 1$, and γ is a constant which is chosen based on the amount of smoothing that is desired in the result. If γ is large, more smoothing is applied, whereas if γ is small, less smoothing is done. Due to the concave nature of the log function, the IPF algorithm has desirable properties: first, the output $\tilde{\lambda}(i,j)$ is strictly positive; second, as the values of $\lambda(i,j)$ become larger, the amount of smoothing is reduced; third, the local means of $\tilde{\lambda}(i,j)$ and $\lambda(i,j)$ are approximately matched.

The ICD updates for this problem take the form:

$$\tilde{\lambda}(m,n) \leftarrow \arg\min_{\tilde{\lambda}(m,n)>0} \left\{ \sum_{m,n} \left(\lambda(m,n) - \tilde{\lambda}(m,n) \right)^2 + \gamma \sum_{(i,j)\neq(m,n)} b_{i-m,j-n} \left(\log\left(\tilde{\lambda}(m,n) \right) - \log\left(\tilde{\lambda}(i,j) \right) \right)^2 \right\}, \tag{21}$$

where $\tilde{\lambda}(m,n)$ is the single detector count element being updated. This update strategy can be applied to each element for a single iteration, and the iterations can be repeated until the desired quality is achieved. Elements are updated in sequential order. Therefore, each time an element is updated, the neighboring elements are affected due to the influence of the second term in equation (21). One could of course imagine applying different penalty function to the different terms of equation (20), or other non-linear functions to replace the logarithms in a manner more representative of the physical conversion from detector counts to attenuation measurements.

In some aspects, the IPF is also similar to the DBS algorithm,[7] in the sense that elements are affected based on their local properties, although it is done here for the specific purpose of correcting positive bias in CT.

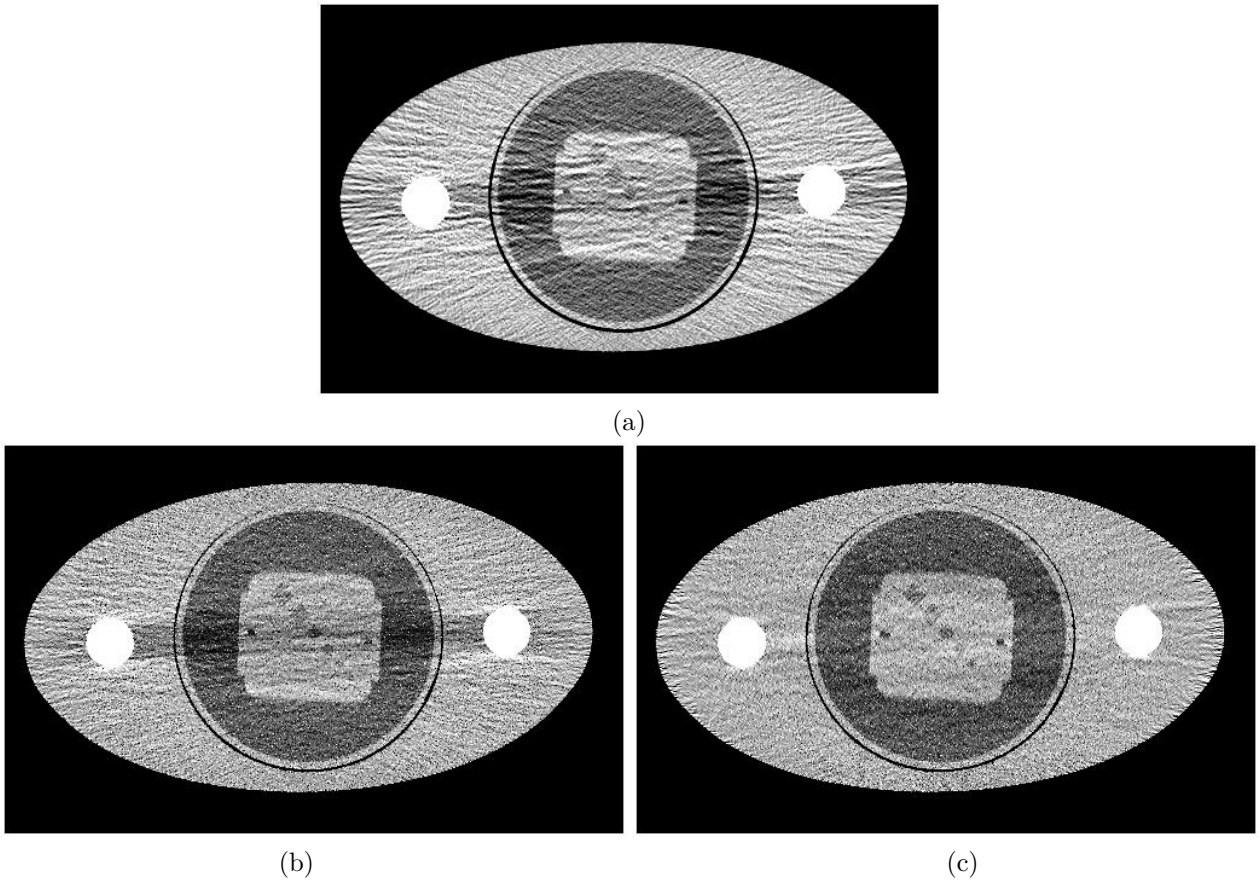

(a)

(b) (c)

Figure 3. Oval phantom with QA insert in 50 cm field of view, 16×0.625mm, 120mA. (a) FBP; (b) IR without MPF nor electronic noise modeling; (c) IR with MPF and electronic noise modeling. Window level 50, window with 350 HU.

5. RESULTS

Both the causal MPF and the non-causal IPF are similar in that they apply an operation that computes the difference between the estimated and actual measurement of detector counts $\lambda(i,j) - \tilde{\lambda}(i,j)$, and propagates this error to neighboring elements in a manner designed to match the local means of $\lambda(i,j)$ and $\tilde{\lambda}(i,j)$. By preserving the mean of the measurement data, the MPF effectively corrects the shading artifacts along the lines of strong attenuation. This is because the MPF reduces or eliminates the bias that would be created by other methods of ensuring the non-negativity of the data processed through the negative logarithm operation of equation (3).

To illustrate these benefits, we scan and reconstruct an oval phantom with a QA insert. The phantom contains Teflon rods on both sides so that horizontal rays through the object are attenuated significantly more than vertical rays, and the susceptibility to quantum detector and photon noise is greater along the horizontal direction. The scan is 16-slice axial with a detector collimation of 0.625 mm, and is acquired at 120 mA to exemplify low-signal cases. The data is pre-corrected for beam hardening based on calibration vectors after the negative logarithm operation is applied, and before the start of image reconstruction. The reconstruction is performed first with FBP with adaptive low-signal correction, using the simple method of taking the absolute value of the negative data in $\lambda(i,j)$ before negative logarithm. Second, iterative reconstruction of the same data without the MPF is done. Figure 3 shows the complete phantom in 50 cm field of view to illustrate the qualitative aspect of the results. The FBP image (a) with adaptive low-signal correction appears at the top. The bottom (b) result is the ICD image without applying the MPF nor modeling electronic noise. We used the GGMRF prior[13] for $U(\mathbf{r})$ with exponent 1.2 in this experiment. Although the ICD image is already significantly

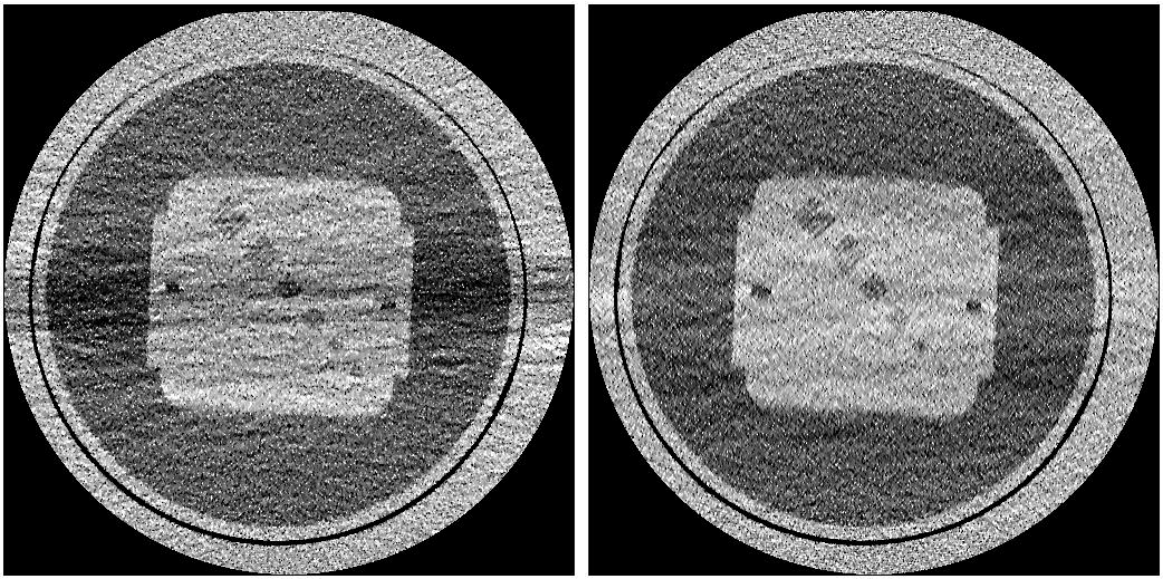

(a) (b)

Figure 4. High resolution image of QA insert in 25 cm field of view. (a) IR without MPF nor electronic noise modeling; (b) IR with MPF and electronic noise modeling. Window level 50, window with 350 HU.

better than the FBP image, the dark noisy horizontal streaks are clearly visible in both uncorrected images. The bottom (c) image is the result of applying both two passes of the MPF, and electronic noise modeling in the iterative loop, to achieve best results.

Figure 4 (a) and (b) show a higher resolution version of the insert in 25 cm field of view with and without the correction, respectively. The positive bias responsible for the shading streaks in the uncorrected image has successfully been compensated by proper handling of the low-signal counts in the data. In addition, the effect of proper electronic noise modeling is to lower the level of confidence in projection data from the photon-starved regions of the sinogram, which are intrinsically unreliable. A risk of such noise modeling that is worth mentioning, with or without MPF for iterative reconstruction, is the non-uniform weighting of projection rays depending on the measured attenuation. The effect of this can be visualized in Figure 4, where it is apparent that the horizontal edges of the QA insert are blurred compared to the vertical edges. The balance between noise weighting in the log-likelihood and the regularization terms in equation (11) needs to be studied further to mitigate the risk.

6. CONCLUSION

We have presented methods to explicitly correct the effects of low-signal data with large quantum and detector noise for computed tomography. Both a causal and a non-causal iterative filter have been introduced for positive bias correction compared to conventional methods. In addition, a model for including electronic noise in the statistical formulation for iterative reconstruction was presented. Phantom results demonstrate positive outcomes. Further advances in the regularization model should address potential issues of non-uniform smoothing in the reconstructions as a result of spatially-varying smoothing in the sinogram.

REFERENCES

1. H. Johns and J. Cunningham, *The Physics of Radiology*, Charles C. Thomas, Springfield, IL, 1983.
2. A. Kak and M. Slaney, *Principles of Computerized Tomographic Imaging*, IEEE Press, New York.
3. J. Hsieh, "Adaptive streak artifact reduction in computed tomography resulting from excessive x-ray photon noise," *Med. Phys.* **25**, pp. 2139–2147, November 1998.

4. D. L. Snyder, C. W. Helstrom, A. D. Lanterman, M. Faisal, and R. L. White, "Compensation for readout noise in CCD images," *J. Opt. Soc. Am. A* **12**(2), pp. 272–283, 1995.
5. J.-B. Thibault, K. Sauer, C. Bouman, and J. Hsieh, "Three-dimensional statistical modeling for image quality improvements in multi-slice helical CT," in *Proc. Intl. Conf. on Fully 3D Reconstruction in Radiology and Nuclear Medicine*, pp. 271–274, (Salt Lake City, UT), July 6-9 2005.
6. R. Floyd and L. Steinberg, "An adaptive algorithm for spatial greyscale," *Journal of the Society for Information Display* **17**(2), pp. 75–77, 1976.
7. M. Analoui and J. Allebach, "Model-based halftoning by direct binary search," in *Proceedings of the SPIE/IS&T Symposium on Electronic Imaging Science and Technology*, **1666**, pp. 96–108, (San Jose, CA), Feb 9-14 1992.
8. R. Gordon and G. Herman, "Three-dimensional reconstruction from projections: A review of algorithms," in *International Review of Cytology*, G. Bourne and J. Danielli, eds., **38**, pp. 111–151, Academic Press, New York, 1974.
9. J.-B. Thibault, K. Sauer, C. Bouman, and J. Hsieh, "Three-dimensional statistical reconstruction for image quality improvements in multi-slice helical CT," *IEEE Trans. on Medical Imaging* , to appear in July 2006.
10. C. Bouman and K. Sauer, "A unified approach to statistical tomography using coordinate descent optimization," *IEEE Trans. on Image Processing* **5**, pp. 480–492, March 1996.
11. K. Sauer and C. Bouman, "A local update strategy for iterative reconstruction from projections," *IEEE Trans. on Signal Processing* **41**, February 1993.
12. B. D. Man, S. Basu, J.-B. Thibault, J. Hsieh, J. Fessler, K. Sauer, and C. Bouman, "A study of different minimization approaches for iterative reconstruction in x-ray CT," in *Proc. of IEEE Nucl. Sci. Symp. and Med. Imaging Conf.*, (San Juan, Puerto Rico), October 23-29 2005.
13. C. Bouman and K. Sauer, "A generalized Gaussian image model for edge-preserving MAP estimation," *IEEE Trans. on Image Processing* **2**, pp. 296–310, July 1993.